1-1-2011

MOCVD of ultra-thin PV solar cell devices using a pyrite based p-i-n structure

Andrew J. Clayton
Glyndwr University, a.clayton@glyndwr.ac.uk

Stuart J. Irvine
Glyndwr University, s.irvine@glyndwr.ac.uk

Vincent Barrioz
Glyndwr University, v.barrioz@glyndwr.ac.uk

W S. Brooks
Glyndwr University

G Zoppi

See next page for additional authors

MOCVD of ultra-thin PV solar cell devices using a pyrite based p-i-n structure

Abstract
Ultra-thin photovoltaic (PV) devices were produced by atmospheric pressure metal organic chemical vapour deposition (AP-MOCVD) incorporating a highly absorbing intermediate sulphurised FeS_x layer into a CdS/CdTe structure. X ray diffraction (XRD) confirmed a transitional phase change to pyrite FeS_2 after post growth sulphur (S) annealing of the FeS_x layer between 400^0C and 500^0C. Devices using a superstrate configuration incorporating a sulphurised or non sulphurised FeS_x layer were compared to p-n devices with only a CdS/CdTe structure. Devices with sulphurised FeS_x layers performed least efficiently, even though pyrite fractions were present. Rutherford back scattering (RBS) confirmed deterioration of the CdS/FeS_x interface due to S inter-diffusion during the annealing process.

Keywords
Ultra thin, PV solar cells, pyrite absorber, metalorganic chemical vapour deposition

Disciplines
Semiconductor and Optical Materials

Authors
Andrew J. Clayton, Stuart J. Irvine, Vincent Barrioz, W S. Brooks, G Zoppi, I Forbes, K D. Rogers, D W. Lane, K Hutchings, and S Roncallo

MOCVD of ultra-thin PV solar cell devices using a pyrite based p-i-n structure

A.J. Clayton[a]*, S.J.C. Irvine[a], V. Barrioz[a], W.S.M. Brooks[a], G. Zoppi[b], I Forbes[b], K.D. Rogers[c], D.W. Lane[c], K. Hutchings[c], S. Roncallo[c].

[a]CSER, Glyndŵr University, OpTIC Glyndŵr, St Asaph, LL17 0JD, UK.
[b]NPAC, Northumbria University, Newcastle upon Tyne, NE1 8ST, UK.
[c]Centre for Material Science and Engineering, Cranfield University, Swindon, SN6 8LA, UK.

*a.clayton@glyndwr.ac.uk; Tel: 44 1745 535213; Fax: 44 1745 535101

Abstract

Ultra-thin photovoltaic (PV) devices were produced by atmospheric pressure metal organic chemical vapour deposition (AP-MOCVD) incorporating a highly absorbing intermediate sulphurised FeS_x layer into a CdS/CdTe structure. X-ray diffraction (XRD) confirmed a transitional phase change to pyrite FeS_2 after post growth sulphur (S) annealing of the FeS_x layer between 400°C and 500°C. Devices using a superstrate configuration incorporating a sulphurised or non-sulphurised FeS_x layer were compared to p-n devices with only a CdS/CdTe structure. Devices with sulphurised FeS_x layers performed least efficiently, even though pyrite fractions were present. Rutherford back scattering (RBS) confirmed deterioration of the CdS/FeS_x interface due to S inter-diffusion during the annealing process.

Introduction

Pyrite and marcasite are two naturally occurring phases of iron disulphide (FeS_2). Marcasite has an orthorhombic structure with a band gap of 0.34 eV making it unsuitable for photovoltaic (PV) applications [1, 2]. Pyrite (FeS_2) has a cubic structure and a high absorption coefficient, which is of the order of 10^5 cm^{-1} in the visible region of the solar spectrum. It has a direct band gap of 0.95 eV reported by Ennaoui and co-workers [3]. This makes it a desirable material for PV applications where photon capture towards the near infrared (NIR) region should be possible; increasing the absorbed photon wavelength range relative to conventional thin film PV cells, such as CdTe. Single phase pyrite films can be obtained by Metal Organic Chemical Vapour Deposition (MOCVD) [4-6] or by annealing Fe [7, 8] or FeS [2] films in a sulphur (S) atmosphere. Ennaoui and co-workers [3] used pyrite in electrochemical PV cells and obtained an efficiency (η) of 2.7%. There were issues with low photovoltages [9,10] which was expected to be related to S deficiency in the pyrite. This paper discusses a feasibility study towards using pyrite as an ultra-thin absorber layer, incorporating it into a CdTe-based device structure developed by Barrioz *et al.* [11] to investigate whether absorption in the device can be enhanced. Thin film PV devices based on the CdS/CdTe junction using a CdTe absorber layer and CdTe:As^+ back contact layer [11] have been optimised [12] to give high efficiency 5 x 5 cm^2 devices with 0.5 x 0.5 cm^2 contacts consistently with η > 10% AM1.5. Parallel research [13] of ultra-thin CdTe PV cells showed that significant values of η >7% AM1.5 can be achieved with CdTe absorber layer thickness ≤1μm. Structures with an intermediate FeS_x layer, sulphurised with S powder in an argon atmosphere, with a p^+ CdTe:As cap layer were produced using the developed atmospheric pressure (AP) MOCVD process [11-13] which is more suitable for scale up than vacuum methods. Gold back contacts, 3.14 x 10^{-2} cm^2 in area, completed the 1.0 x 2.0 cm^2 device structures and results of device performance are reported.

Experimental

AP-MOCVD was used to deposit FeS_x onto aluminosilicate glass using a horizontal quartz reactor tube. Iron pentacarbonyl ($Fe(CO)_5$) was used in combination with tertiarybutyl thiol (t-BuSH) or diethyl disulphide (Et_2S_2) to control the rate of reaction and the film stoichiometry. The quartz reactor chamber was heated up to 500°C by a 1kW infrared heater using a thermocouple inserted into a groove under the graphite susceptor for temperature control. Precursor partial pressures were controlled to give S/Fe ratios of 400. The as-grown layers were S deficient and post growth annealing in a S atmosphere converted FeS_x to pyrite FeS_2. Devices were made incorporating an intermediate sulphurised or non-sulphurised FeS_x layer between CdS and CdTe to form a p-i-n structure. Structures with only the CdS/FeS_x interface were also assessed using a sulphurised 200 nm FeS_x layer.

Results and Discussion

X-ray diffraction (XRD) characterisation showed that the films were predominantly FeS or $Fe_{1-x}S$ phases for all MOCVD growth temperatures ranging from 180°C to 500°C. A temperature of 300°C was used for all depositions onto CdS due to parasitic deposition inside the injector at higher temperatures. A transitional phase change to pyrite FeS_2 after post-growth sulphurisation from 400°C was confirmed by XRD characterisation. This is in agreement with observations by Zheng and co-workers [2]. *Fig. 1* shows proportional XRD peak intensity for the different phases comparing FeS_x layers deposited onto CdS by MOCVD at 300°C that have been sulphurised at different temperatures between 400°C and 500°C. It can be observed that conversion to pyrite increases from 400°C to 450°C. The anneal soak time for sulphurisation had a more significant effect, where annealing for 30 minutes resulted in a greater conversion to pyrite than a 10 minute anneal. No change in the pyrite fraction was observed by increasing the temperature from 450°C to 500°C. Zheng and co-workers [2] found 500°C to be the optimum temperature and observed single phase pyrite when using 10 hour soak times. The relative rates of S inter-diffusion between the CdS/FeS_x interface at 450°C and 500°C may differ, masking the effect of sulphurisation.

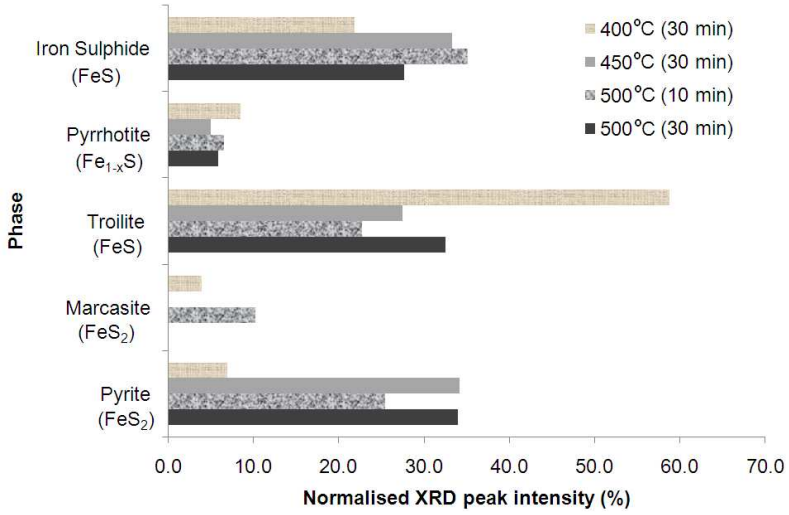

Fig. 1: Normalised XRD peak intensities to show proportional phases present in MOCVD FeS_x layers on CdS after sulphurisation at temperatures 400°C - 500°C.

Transmittance (T%) spectra of FeS_x layers with average thickness around 100 nm deposited onto glass substrates were observed to be highly absorbing, becoming more absorbent in the visible region but extending, as expected, well into the IR. Sulphurisation of the FeS_x layers significantly increased absorbance in the visible region, such that nearly all of the visible light was absorbed. This was also observed for sulphurised FeS_x around 200nm in thickness, deposited onto a 240 nm CdS layer on ITO coated aluminosilicate

substrates. *Fig. 2* shows T% spectra for equivalent CdS/FeS_x layers sulphurised at temperatures ranging between 400°C and 500°C, with two samples sulphurised at 500°C with different soak times. The spectra show increased absorbance with temperature towards longer wavelengths. This implies greater pyrite fraction which correlates with observations from Zheng's group [2] where the pyrite fraction increased at 500°C with longer anneal time.

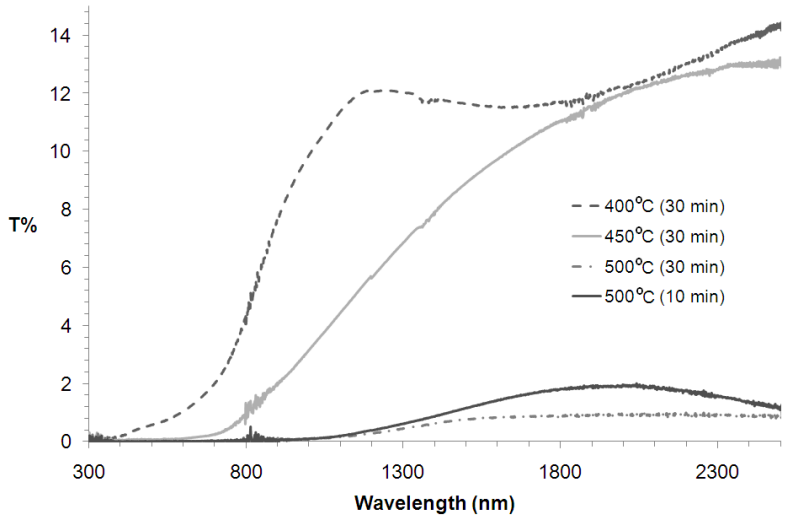

Fig. 2: Comparison of Transmittance spectra of FeS_x deposited onto CdS at 300℃ by MOCVD with post-sulphurisation at temperatures 400℃ - 500℃.

Ultra-thin film devices adopting the CdTe superstrate configuration were produced incorporating either an FeS_x layer as-grown by MOCVD or including S annealing post-growth between a 250 nm CdTe:As^+ layer and a 240 nm CdS n-type layer, deposited onto ITO coated aluminosilicate glass substrates. These devices were compared to CdS/CdTe structures without FeS_x. Mean results from *I/V* measurements from 6-8 contacts, depending on the device, for selected samples that gave best efficiencies (η) are displayed in *Table 1*. Thicknesses of Fe films before and after S annealing were reported [7, 8] to increase after sulphurisation, which was carried out for up to 20 hours. In this study however, the sulphurised FeS_x layer thickness was assumed to be the same as the equivalent S deficient as-grown layers, as sulphurisation was only carried out for up to 30 minutes.

Sample	Jsc (mA/cm^2)	Voc (mV)	η %	FF %	FeS_x (nm)
t-BuSH (no S anneal)	10.77	498.33	2.82	52.25	99.50
Std. Dev.	0.68	10.33	0.38	4.08	30.41
t-BuSH (S anneal)	6.26	221.84	0.60	31.90	99.50
Std. Dev.	1.87	113.38	0.36	15.75	30.41
t-BuS_2S_2 (no S anneal)	8.38	318.13	1.46	39.89	53.50
Std. Dev.	3.00	179.47	0.92	18.56	123.74
t-Bu_2S_2 (S anneal)	3.12	179.80	0.20	32.38	53.50
Std. Dev.	1.91	60.51	0.19	3.79	123.74
p-n device 2	10.36	394.00	2.38	52.67	0.00
Std. Dev.	1.07	183.86	1.16	10.63	
p-n device 1	10.63	251.29	1.02	28.89	0.00
Std. Dev.	2.54	168.96	0.84	14.66	

Table 1: Averaged I/V results for devices with sulphurised and non-sulphurised FeS_x layers, and for p-n devices without a FeS_x layer.

The best performing device with lowest standard deviation (σ) for short circuit current (J_{sc}), open circuit voltage (V_{oc}) and efficiency (η) incorporated a non-sulphurised FeS_x layer. Comparison of this device with the p-n devices without FeS_x showed little difference in the calculated mean J_{sc}, even though σ was larger for the p-n structures. The J_{sc} was higher in these devices than the majority of structures incorporating FeS_x, suggesting lower carrier recombination in the p-n structure. This implies that the presence of the FeS_x layer is creating a high concentration of deep traps compared with the CdS/CdTe junction.

The V_{oc} is significantly reduced for the p-n structure relative to the best device with intermediate FeS_x layer. The p-n structures had the same CdS and CdTe:As^+ layer thickness and were therefore thinner than the devices incorporating FeS_x. Ultra-thin devices typically suffer from pin holes and other defects that can cause shunts which will reduce the V_{oc}. This is reflected in the large σ for V_{oc} for these p-n structures which may be a result of pinhole defects. Inclusion of the FeS_x layer may help to reduce these shunt paths due to its high impedance, which will be reflected in a higher V_{oc}.

Spectral quantum efficiency (QE) was measured for some of the device samples represented in *Table 1* and the results of the characterisation are shown in *Fig. 3*. The p-n structure shows the greatest variation in QE from different contacts on the same device, which demonstrates large lateral inhomogeneity in the absence of an FeS_x layer. The conversion efficiencies were slightly improved for the non-sulphurised p-i-n structure suggesting that the S deficient FeS_x layer was contributing the junction, which reflects the higher V_{oc} for this device. The larger absorption of the sulphurised FeS_x layers observed in T% spectra was not replicated in the QE characterisation of the devices. This also correlates with the poorer results from *I/V* measurements for the devices with sulphurised FeS_x layers compared to those with as-grown FeS_x

layers. This is reflected in the characteristic photon conversion cut-off around 850 nm for CdTe–based devices.

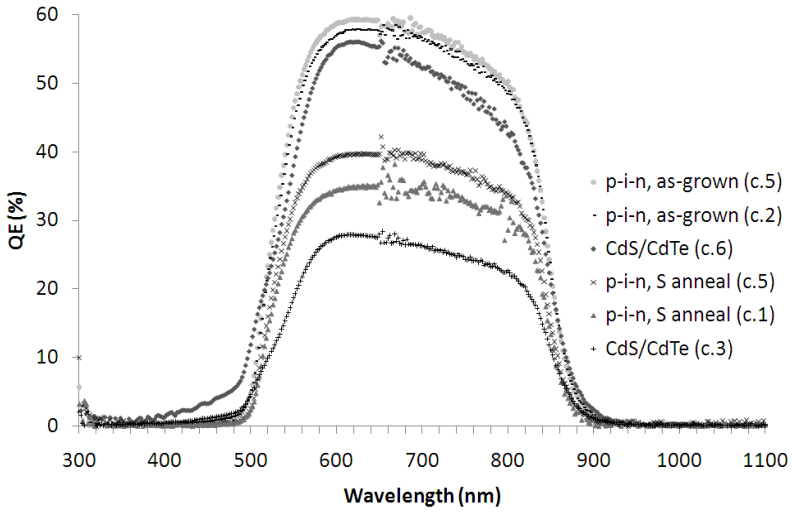

Fig. 3: QE characterisation of different contacts from devices incorporating FeS_x layers with and without S annealing, and for a p-n structure without the FeS_x layer.

The *I/V* and QE results strongly suggest that S inter-diffusion was occurring during sulphurisation which is carried out at higher temperature than the MOCVD process. This phenomenon was investigated by subjecting 3 samples to temperature cycling, mimicking growth steps of the CdTe layer (parameters listed below) where higher temperature steps are employed.

a) As-grown CdS/FeS_x at 300°C;
b) CdS/FeS_x cycled at 390°C for 40 mins;
c) CdS/FeS_x cycled at 390°C for 40 mins followed by 420°C for 10 mins.

The stoichiometry of CdS and FeS_x in the CdS/FeS_x structure of each sample was then characterised using rutherford back scattering (RBS). The results for each sample determined from the RBS measurements are displayed in *Table 2*.

		(a)	(b)	(c)
FeS	**S**	0.50	0.46	0.28
	Fe	0.50	0.54	0.72
CdS	**S**	0.50	0.44	0.75
	Cd	0.50	0.56	0.25

Table 2: Stoichiometry results from RBS measurements of: (a) As-grown FeS_x layer by MOCVD at 300℃; (b) As-grown layer with temperature cycle for 40 min. after stabilisation at 390℃; (c) As-grown layer with temperature cycle after stabilisation for 40 min. at 390℃ and 10 min. at 420℃.

The ratio of Fe:S for the FeS_x layer and Cd:S for the CdS layer is approximately 1:1 for the as-grown sample (a) and for sample (b) that went through the temperature cycle at 390°C. However, it can be observed for sample (c) a shift in ratio for S occurred in both the FeS_x and CdS layers. The results show that diffusion of S between the layers is occurring at temperatures above 400°C. This demonstrates the CdS/FeS_x junction deteriorates during sulphurisation reflecting the decreased performance for devices incorporating a sulphurised FeS_x layer, even with pyrite present. The CdS/FeS_x interface will have to remain intact to enable comprehensive assessment of a thin film PV device containing pyrite. A device adopting a substrate configuration needs to be considered, where the FeS_x layer is deposited and sulphurised before the CdS window layer. This will remove limitations associated with the superstrate configuration where S inter-diffusion hinders device performance.

Conclusion

The inclusion of a thin FeS_x layer between the CdS/CdTe junction was observed to significantly improve the V_{oc} for the best performing p-i-n device compared to the p-n structures. The p-n structures suffered from reduced V_{oc} which is likely to be due to pinholes in this very thin structure. However, incorporating FeS_x has not yet proved to be successful in enhancing the J_{sc}, where only the best performing p-i-n device incorporating a non-sulphurised FeS_x layer had similar J_{sc} to the p-n device structures. This demonstrated a better defined interface at the p-n junction relative to the majority of the p-i-n structures where the J_{sc} values were significantly higher than for devices incorporating sulphurised FeS_x layers. RBS results demonstrated S inter-diffusion to occur in CdS/FeS_x samples at temperatures >400°C, causing deterioration of the CdS/FeS_x junction. This implicates the limitation of sulphurisation using the superstrate configuration that has been employed for these devices and reflects the reduction in device performance of p-i-n structures with FeS_x layers that have been through S annealing. As a result, structures containing pyrite have not shown the anticipated contribution to device performance suggesting the major active layer in the device was the 250 nm thick CdTe:As^+ layer, as supported by characteristic CdTe absorption in QE. Control of the interfaces and inter-diffusion of S to avoid carrier recombination in the FeS_x layer is necessary. A device structure based on FeS_x/CdS utilising the substrate configuration with pyrite layer deposited onto a substrate employed as the back contact with subsequent CdS layer growth may provide a more suitable route towards using pyrite as an absorber layer in a thin film PV device.

References

[1] S. Nakamura and A. Yamamoto, *Solar Energy Mat. & Solar Cells* 65 (2001) 79.

[2] Y.Z. Dong, Y.F. Zheng, H. Duan, Y.F. Sun and Y.H. Chen, *Mat. Lett.* 59 (2005) 2398.

[3] A. Ennaoui, S. Fiechter, C. Pettenkofer, N. Alonso-Vante, K. Büker, M. Bronold, C. Höpfner and H. Tributsch, *Solar Energy Mat. & Solar Cells* 29 (1993) 289.

[4] D.M. Schleigh and H.S.W. Chang, *J. Crystal Growth* 112 (1991) 737.

[5] B. Meester, L. Reijnen, A. Goossens and J. Schoonman, *Chemical Vapour Deposition* 6 (2000) 121.

[6] C. Höpfner, K. Ellmer, A. Ennaoui, C. Pettenkofer, S. Fiechter and H. Tributsch, *J. Crystal Growth* 151 (1995) 325.

[7] J.R. Ares, A. Pascual, I.J. Ferrer and C. Sánchez, *Thin Solid Films* 480-481 (2005) 477.

[8] Y.H. Liu, L. Meng and L. Zhang, *Thin Solid Films* 479 (2005) 83.

[9] K. Ellmer and H. Tributsch, *Proc. 12th Quantum Solar Energy Conversion Workshop, Wolkenstein, Südtrirol, Italy*, 2000.

[10] A. Ennaoui, S. Fiechter, W. Jaegermann and H. Tributsch, J*. Electrochem. Soc.* 133 (1986) 97.

[11] V. Barrioz, Y. Proskuryakov, E.W. Jones, J. Major, S.J.C. Irvine, K. Durose and D. Lamb, *Mat. Res. Soc. Symp. Proc*. (2007), 1012, Y12-08.

[12] S.J.C. Irvine, V. Barrioz, D. Lamb, E.W. Jones and R.L. Rowlands-Jones, *J. Crystal Growth* 310 (2008) 5198.

[13] E.W. Jones, V. Barrioz, S.J.C. Irvine and D. Lamb, *Thin Solid Films* 517 (2009) 2226.

Acknowledgements

The authors are grateful to the EPSRC funded PV Supergen Consortium for supporting this research and to SAFC Hitech for supplying the precursors.